Computerized Medical Imaging and Graphics xxx (2013) xxx–xxx

Contents lists available at SciVerse ScienceDirect

Computerized Medical Imaging and Graphics

journal homepage: www.elsevier.com/locate/compmedimag

Detection of neovascularization in retinal images using multivariate *m*-Mediods based classifier

M. Usman Akram [a,*], Shehzad Khalid [b], Anam Tariq [a], M. Younus Javed [a]

[a] Department of Computer Engineering, College of Electrical and Mechanical Engineering, National University of Sciences & Technology, Pakistan
[b] Department of Computer & Software Engineering, Bahria University, Pakistan

ARTICLE INFO

Article history:
Received 11 December 2012
Received in revised form 26 June 2013
Accepted 29 June 2013

Keywords:
Retinal image analysis
Blood vessels
Neovascularization
Proliferative diabetic retinopathy
Mediods

ABSTRACT

Diabetic retinopathy is a progressive eye disease and one of the leading causes of blindness all over the world. New blood vessels (neovascularization) start growing at advance stage of diabetic retinopathy known as proliferative diabetic retinopathy. Early and accurate detection of proliferative diabetic retinopathy is very important and crucial for protection of patient's vision. Automated systems for detection of proliferative diabetic retinopathy should identify between normal and abnormal vessels present in digital retinal image. In this paper, we proposed a new method for detection of abnormal blood vessels and grading of proliferative diabetic retinopathy using multivariate *m*-Mediods based classifier. The system extracts the vascular pattern and optic disc using a multilayered thresholding technique and Hough transform respectively. It grades the fundus image in different categories of proliferative diabetic retinopathy using classification and optic disc coordinates. The proposed method is evaluated using publicly available retinal image databases and results show that the proposed system detects and grades proliferative diabetic retinopathy with high accuracy.

1. Introduction

Diabetic retinopathy (DR) is a progressive eye disease that is caused by the increase of insulin in the blood and can cause blindness if not detected timely [1]. DR is also caused by the microvascular complication of diabetes and it is one of the main sources of vision impairment. A number of studies have shown that DR is one of the major causes of blindness in industrialized countries [2]. One out of five patients with newly discovered type II diabetes has DR at the time of diagnosis, where DR almost never occurs in first five years after diagnosis of type I diabetes [1]. The common symptoms of diabetic retinopathy are blurred vision, floaters and flashes, and sudden loss of vision [3].

Healthy retina contains blood vessels, optic disc (OD), macula and fovea as main components [2] whereas an affected retina may also contain different signs of DR. DR is broadly divided into two stages i.e. non proliferative diabetic retinopathy (NPDR) and proliferative diabetic retinopathy (PDR). NPDR also known as background DR contains the early signs of presence of DR such as microaneurysms and dot haemorrhages caused by the breaks in tiny small vessels called capillaries [4]. As the disease progresses, more signs of DR appear such as hard and soft exudates which are caused by the leakage of fats and proteins on the surface of retina known as severe NPDR. PDR is an advanced stage of DR and it is divided into two stages; i.e. neovascularization on optic disc (NVD) and neovascularization elsewhere (NVE) [4]. In PDR, retina sends signals for nourishment of oxygen deprived areas. As a result of this, new blood vessels start growing in different regions of retina to supply blood which is a good thing but these new vessels are weak and their walls are thin and fragile. These infant vessels may easily start leaking blood on surface of retina and cause severe vision loss, even blindness [5]. Fig. 1 shows digital images of healthy retina and retina affected with PDR.

Digital retinal images are used in computer aided diagnostic (CAD) systems for screening of DR and its different stages. Different signs of NPDR and PDR appear with different properties on the surface of retina and it is the goal of CAD systems to identify these signs for timely and accurate treatment of DR. A number of fundus image databases are publicly available for the purpose of evaluation and testing of proposed systems for the diagnosis of retinal diseases. Fig. 2 shows digital images of healthy retina and retina affected with PDR.

A number of computer aided diagnostic systems have been proposed in literature for early detection of DR and lesions related to NPDR [6–10]. All these systems covered early signs of DR such as microaneurysms and exudates. Although it is important to detect DR at its early stage, however early detection of PDR is also very important to save patient's vision. Only a few studies have been

* Corresponding author. Tel.: +92 3336913921
E-mail address: usmakram@gmail.com (M. Usman Akram).

0895-6111/$ – see front matter © 2013 Elsevier Ltd. All rights reserved.
http://dx.doi.org/10.1016/j.compmedimag.2013.06.008

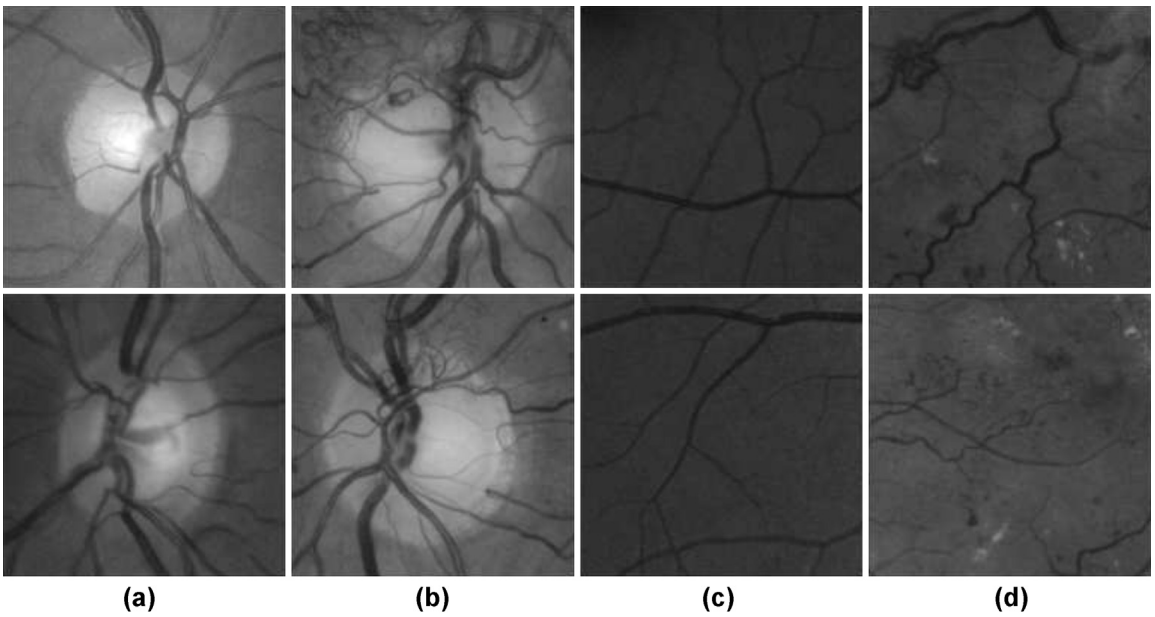

Fig. 1. Normal and abnormal blood vessel structures: (a) optic disc with normal vessel; (b) optic disc with abnormal vessels (NVD); (c) normal vascular structure; (d) abnormal vessels other than OD (NVE).

carried out on PDR. Goatman et al. [11] proposed a method for automatically detecting new vessels on the optic disc by detecting blood vessels and using support vector machine to categorize a vessel segment as normal or abnormal. They presented a good set of features to detect neovascularization but limited their scope with NVD only. This limitation makes it relatively easy to detect abnormal vessels from a specific region of interest instead of looking for abnormal vessels from whole image. A multiscale amplitude-modulation–frequency-modulation (AM–FM) based method for discriminating between normal and pathological retinal images containing neovascularization was presented in [12]. They used only 120 regions from just 15 images with different DR signs and classified those signs into different categories. A study on 27 fluorescein angiogram images was done by Jelinek et al. [13] to examine vascular pattern characteristics to detect PDR. Nayak et al. presented a simple artificial neural network based method for detection of PDR with help of just blood vessel area and perimeter [14]. A small database of 36 images was used and they achieved 90.91% accuracy. Although [12] and [14] have presented the methods for neovascularization, they focused a little bit on accurate extraction of blood vessels which is the core for detection of abnormal vessels.

Computer aided diagnostic system for PDR should be able to detect blood vessels accurately. A number of methods have been proposed for blood vessel detection and segmentation [15–19], but detection of neovascularization is still a difficult problem. Blood vessel extraction algorithms normally contain two parts, first is enhancement of blood vessels and second is the segmentation and classification of vessel pixels. Chaudhuri et al. [18] proposed a matched filter based method for blood vessel detection and it has been widely used for extraction purposes but it has been unable to find small blood vessels. Later, a threshold probing based technique was presented in [19] to improve the accuracy of matched filters. They analyzed the region based features of vessel structure. Mendonca et al. [20] used a first order derivative of Gaussian filter and a modified top hat operator for blood vessel enhancement and segmentation. Another probing algorithm using multithresholds was presented in [21].

The existing methods which we have discussed here with respect to neovascularization consist of different limitations such as (i) very little focus is given to accurate blood vessel segmentation, (ii) only few of them have extracted reliable features for detection of abnormal vessels, (iii) NVE and NVD are not detected collectively using a common method, and (iv) the classification stage is not

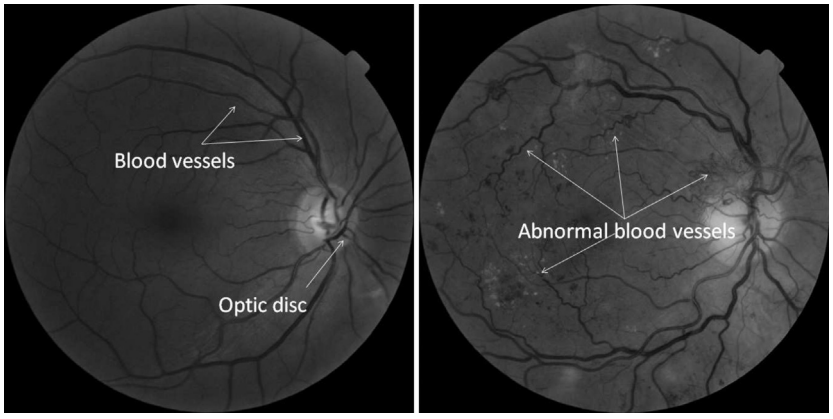

Fig. 2. Digital fundus image: left is normal retinal image with blood vessels and optic disc. Right image contains abnormal blood vessels.

Please cite this article in press as: Usman Akram M, et al. Detection of neovascularization in retinal images using multivariate *m*-Mediods based classifier. Comput Med Imaging Graph (2013), http://dx.doi.org/10.1016/j.compmedimag.2013.06.008

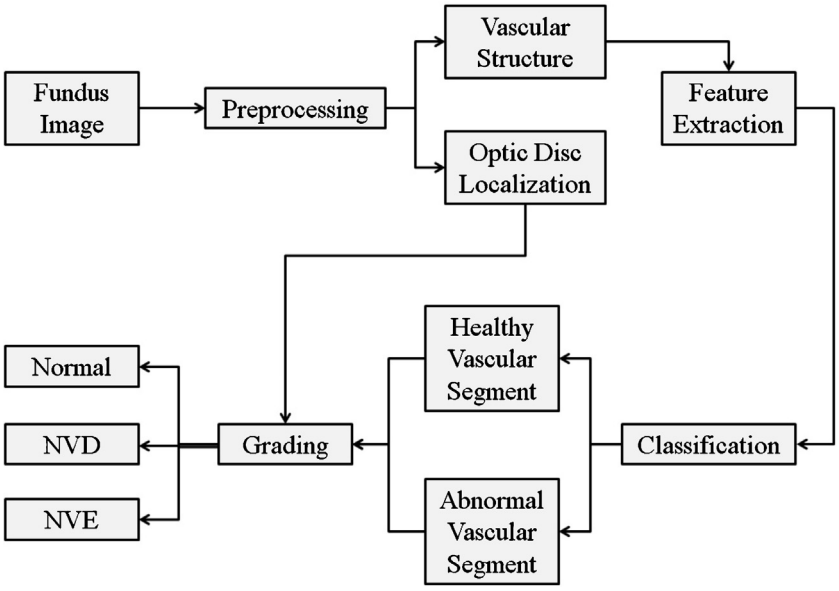

Fig. 3. Flow diagram for proposed multilayered thresholding technique for blood vessel segmentation.

given any proper focus and it is done by using existing SVM or neural network. In contrast to all these limitations, we propose a complete new system for PDR detection and grading which is very rare in literature. Main contributions of proposed system are representation of abnormal vessels with detailed feature set and the use of new dynamic modeling technique for detection of abnormal vessels using multivariate *m*-Mediods based classifier. We propose a new set of features to differentiate between normal and abnormal blood vessels and combine it with OD detection to grade the fundus image in different categories of PDR.

The rest of the paper is organized as follows: Section 2 describes the proposed system and its all phases in detail. The evaluation of proposed system using different retinal image databases and performance parameters is done in Section 3 followed by conclusion in last section.

2. Proposed method

Proliferative diabetic retinopathy (PDR) is an advance stage which can lead to severe vision impairments. Automated systems with accurate detection of PDR are of great significance for in time detection and treatment of PDR to save patient's vision. We present a computer aided diagnostic system for detection of abnormal blood vessels and grading of PDR. In start, the system performs preprocessing, blood vessel segmentation and optic disc localization. A detailed feature set to differentiate between normal and abnormal vascular segments is extracted using different features. We propose a new multivariate *m*-Mediods based modeling and classification approach for accurate classification of vascular segments. Finally, the system grades the fundus image as normal, NVD and NVE using OD coordinates and output of classification process. Fig. 3 shows a flow diagram of proposed system for detection of neovascularization.

2.1. Preprocessing

A digital color retinal image consists of a (semi) circular region of interest on a dark background. This dark background is initially never really black. It is important to distinguish between background and foreground, because feature extraction and abnormality detection algorithms only need to consider the foreground pixels. So it is necessary to remove the foreground from background. At the preprocessing stage, we create binary masks for background and noisy areas. The details regarding preprocessing method are given in [24]. Fig. 4(b) shows binary preprocessing mask for input fundus image.

2.2. Optic disc (OD) localization and detection

NVD is one stage in PDR in which new abnormal blood vessels start growing on optic disc so it is important for automated system

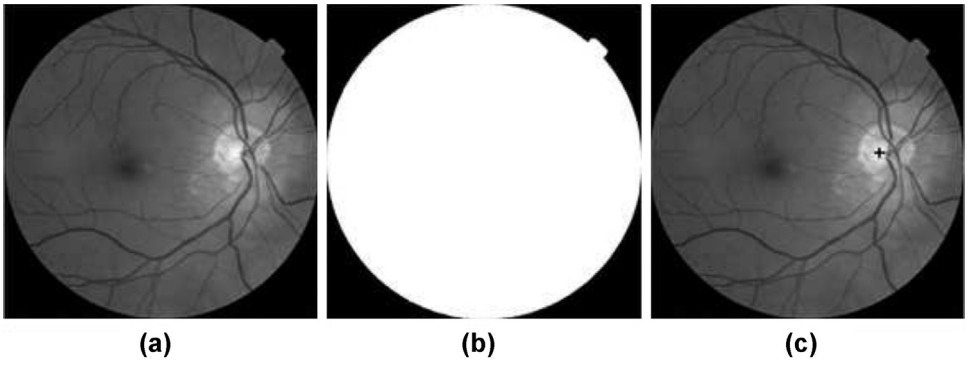

Fig. 4. (a) Digital fundus image, (b) background mask, and (c) optic disc localization.

Please cite this article in press as: Usman Akram M, et al. Detection of neovascularization in retinal images using multivariate *m*-Mediods based classifier. Comput Med Imaging Graph (2013), http://dx.doi.org/10.1016/j.compmedimag.2013.06.008

to locate OD prior to classify PDR as NVD or NVE. OD appears as bright circular or elliptic region on fundus image and blood vessels originate from it. In the proposed system, OD is localized and segmented using averaging filter and circular Hough transform [25]. In OD localization, first original retinal image is preprocessed by averaging mask of size 31×31 in order to remove the background and lesion artifacts which can cause false localization and then maximum gray values from image histogram is detected because the gray values of OD are higher than the background values. Fig. 4(c) shows localized OD in fundus image.

2.3. Vascular pattern extraction

The last step in first phase of proposed system is vascular pattern extraction. It consists of vessel enhancement and segmentation.

2.3.1. Blood vessel enhancement

PDR is identified by the development of new abnormal blood vessels, so it is very important to extract the vascular pattern accurately. The vessels vary in terms of structure, shape and size so it is difficult to extract them. Thin blood vessels or capillaries are less visible than the normal blood vessels and require enhancement before extraction. Most of the times, matched filters (MFs) [18] are used for blood vessel enhancement but the drawback is that MFs not only enhance blood vessel edges but also enhance bright lesions. On the other hand, Gabor wavelets can be tuned for specific frequencies and orientations which is useful for both thick and thin vessels [22]. We have applied the Gabor wavelet using 2D continuous time wavelet transformation (CWT). The 2D CWT $W_\Phi(\mathbf{b}, \theta, a)$ is defined in terms of the scalar product of $g(x, y)$ with the transformed wavelet $\Phi_{\mathbf{b},\theta,a}(\mathbf{x})$

$$W_\Phi(\mathbf{b}, \theta, a) = C_\Phi^{-1/2} a \int \exp(j\mathbf{Rb})\hat{\Phi}^*(ar_{-\theta}\mathbf{R})\hat{g}(\mathbf{R})d^2\mathbf{R} \quad (1)$$

where $j = \sqrt{-1}$ and the hat ($\hat{\Phi}$) denotes a Fourier transform. C_Φ, Φ^*, $\mathbf{b}$, θ and a denote the normalizing constant, complex conjugate of Φ, the displacement vector, the rotation angle, and the dilation parameter respectively. $r_{-\theta}$ is two dimensional rotation along $\mathbf{x}$.

The mathematical functions for Gabor wavelet and its Fourier transform are defined as

$$\Phi_G(\mathbf{x}) = \exp(j\mathbf{R}_0\mathbf{x}) \exp\left(-\frac{1}{2}|\mathbf{Ax}|^2\right) \quad (2)$$

$$\hat{\Phi}_G(\mathbf{x}) = (detA^{-1})^{1/2} \exp\left(-\frac{1}{2}(A^{-1}(\mathbf{R} - \mathbf{R}_0)^2)\right) \quad (3)$$

Here $\mathbf{x} = [xy]^T$ and $\mathbf{R}_0$ is a vector that defines the frequency of the complex exponential. $A = \begin{bmatrix} \epsilon^{-1/2} & 0 \\ 0 & 1 \end{bmatrix}$ with elongation $\epsilon \geq 1$ is a 2×2 positive definite diagonal matrix which defines the wavelet anisotropy and elongation of filter in any desired direction.

For each pixel position with fixed values of $\mathbf{b}$ and a, the Gabor wavelet transform $W_\Phi(\mathbf{b}, \theta, a)$ is computed for θ spanning from 0° up to 165° at steps of 15° and the maximum is taken.

$$M_\Phi(\theta) = max|W_\Phi(\mathbf{b}, \theta, a)| \quad (4)$$

The scale value is different for different databases and is calculated empirically for each database.

2.3.2. Blood vessel segmentation

The wavelet transformation enhances the blood vessels by giving high responses for vascular areas but still thick vessels have high wavelet response as compare to thin vessels. So it is hard to find one optimal threshold value for accurate vascular extraction without any supervised algorithm. This is of great importance especially in case of PDR as new abnormal blood vessels are normally very thin. We presented a recursive supervised multilayered thresholding-based method for accurate vascular segmentation [23]. The algorithm starts with an initial threshold value T using histogram of wavelet image such that it only keeps those pixels for which wavelet response is higher than T. Next step performs vessel thinning using morphological operation [26] and finds edges by applying crossing number method given in equation

$$E(p) = \frac{1}{2}\sum_{i=1}^{8} |f(p_{imod8}) - f(p_{i-1})| \quad (5)$$

where p_0–p_7 are the pixels belonging to a clockwise ordered sequence of pixels defining the 8-neighborhood of p and $f(p)$ is the pixel value in thinned image. $f(p) = 1$ for vessel pixels and zero elsewhere. $E(p) = 1$ and $E(p) = 2$ correspond to vessel edge point and intermediate vessel point respectively. In next iteration, it lowers the threshold and keeps those vascular segments which are connected to the ones obtained in previous iteration. Following steps are then performed iteratively.

1 Compute thinned blood vessels by taking segmented blood vessels as a input.
2 Find out all vessel edges by removing false edges, small segments and validating the edges.
3 Calculate the difference image by subtracting the current thinned vessel image from the one obtained in previous iteration. Only keep those segments which are connected to vessel edges. If new added vessel segments are more than $T_{segment}$ pixels add them. The value of $T_{segment}$ is different for each database and is calculated empirically.
4 If no vessel segment is added, stop iteration otherwise set $T = T - 1$ and repeat steps 1–4.

The algorithm stops when there is not any significant change in vessels during two consecutive iterations. Final segmented image is used to create a gray level segmented image which contains selected blood vessels only with their original intensity values. An adaptive threshold is further applied to improve the segmentation accuracy and to generate a binary mask for blood vessel segmentation. Fig. 5 shows the flow diagram of proposed multilayered thresholding technique for vascular pattern segmentation.

Fig. 6 shows enhanced and segmented vascular patterns after the application of wavelet and multilayered thresholding. Vessel segmentation step makes sure that only true vessels are added in vascular pattern. The false structures which arises due to presence of any DR lesions such as microaneurysms, haemorrhages and exudates etc are removed by checking their connectivity with true vessels. Fig. 6 also shows the vascular pattern extracted by using multilayered thresholding technique in the presence of different DR lesions.

2.4. Feature set formulation

An automated system needs some properties of normal and abnormal blood vessels in order to distinguish between them. Abnormal blood vessels appear as a denser group of vessels and they normally are in form of small vascular segments. Vascular extraction stage tries to find as many blood vessel as it can so that small and thin blood vessel can also be included in classification stage. For an automated system to distinguish between healthy and unhealthy vascular segments, a feature set is formed for each candidate segment. Here the blood vessels are the general vessels which appear in fundus images. Blood vessel segments or vascular segments mean a specific portion of blood vessel which lies within a region of interest which is a square window of size $w \times w$ and w

Please cite this article in press as: Usman Akram M, et al. Detection of neovascularization in retinal images using multivariate m-Mediods based classifier. Comput Med Imaging Graph (2013), http://dx.doi.org/10.1016/j.compmedimag.2013.06.008

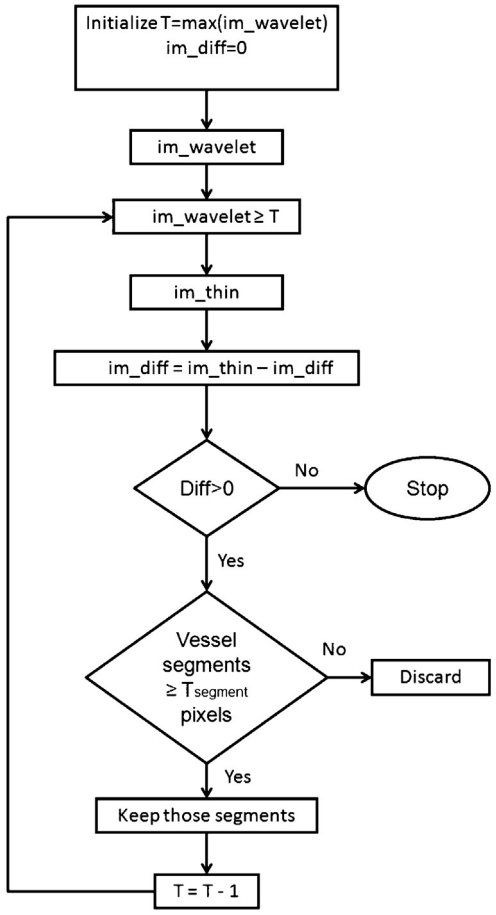

Fig. 5. Flow diagram for proposed multilayered thresholding technique for blood vessel segmentation.

is calculated empirically for each database such that it captures all local variations in a vessel. Candidate segment is blood vessel segment which is currently under consideration for feature extraction or classification.

Each candidate segment is considered as sample for classification and represented by a feature vector. If a retinal image χ contains k candidate blood vessel segments, then the set representation for an image χ is $\chi = \{\upsilon_1, \upsilon_2, \upsilon_3, \ldots, \upsilon_k\}$ where υ_j is a feature vector for jth candidate segment containing m features i.e. $\upsilon = \{x_1, x_2, x_3, \ldots, x_m\}$. The motivation behind these features is that neovascularization (abnormal vessels) always occur in form of bunches and they are more in density and localized within a specific window, which is calculated empirically, as compared to normal vessels. The description of features we have used for classification of healthy and unhealthy vascular segments are as following:

Area (x_1): The sum of vascular pixels inside a square window. Normal blood vessels are thicker than abnormal vessels.
Energy (x_2): The square of intensities of vessel pixels within candidate segment. Healthy vessels are normally brighter than unhealthy vessels in the inverse green channel.
Mean gradient (x_3): The mean value of gradient magnitude of vessels within candidate segment.
Standard deviation gradient (x_4): The standard deviation of vessel gradient magnitude within candidate segment.
Mean intensity (x_5): The normalized mean intensity value of candidate segment. It is computed by first normalizing the intensity values in candidate segment by subtracting the mean from intensity values and then dividing by the standard deviation. Final mean intensity is the mean value of normalized intensities.
Intensity variation (x_6): It is the ratio of mean and standard deviation value of intensity for candidate segment.
Vessel segments (x_7): It measures the total number of vessel segments within candidate segment. Abnormal vessels normally have more segments than normal vessels. This feature is measured using connected component analysis.

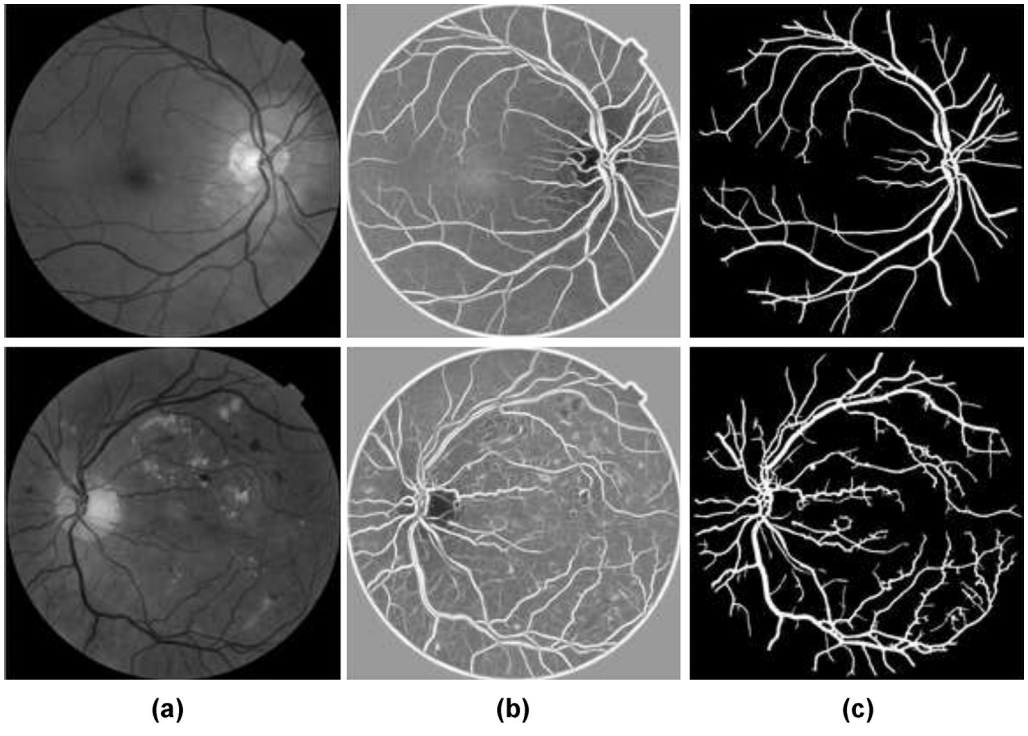

Fig. 6. (a) Digital fundus image, (b) wavelet based enhanced vascular structure, and (c) binary vascular mapped extracted using multilayered thresholding technique.

Please cite this article in press as: Usman Akram M, et al. Detection of neovascularization in retinal images using multivariate m-Mediods based classifier. Comput Med Imaging Graph (2013), http://dx.doi.org/10.1016/j.compmedimag.2013.06.008

Blood vessel density (x_8): It measures the blood vessel density within candidate segment. It is useful because abnormal blood vessel are denser than normal blood vessels. It is computed by dividing total number of segments by window size i.e. $x_8 = x_7/w^2$.
Vascular segment width (x_9): The width of vascular segments within a square window is computed using edge direction and transition in binary values. Fragile vessels normal have small width as compare to normal ones.
Vascular direction variation (x_{10}): The mean value of change in vascular segment direction. Abnormal vessels appear as irregular structure which normally have large value of mean variation in segment direction.

2.5. Modeling and classification of vascular segments

In this section, we present our proposed classification approach for effective modeling and recognition of abnormal vascular patterns. The proposed classification approach enhances feature space representation by employing supervised transformation to increase intra class similarity and reduce intra-class similarity. This is achieved by applying a supervised local Fisher discriminant analysis (LFDA) which identifies principal directions in the feature space that results in maximized discrimination between different classes. More formally, let $DB = \{v_1, v_2, \ldots, v_n\}$ be a set of n training samples belonging to c vascular classes $\{Normal, Abnormal\}$. The within class and between class scatter matrix is computed as:

$$\aleph_w = \frac{1}{2}\sum_{i=1}^{n}\sum_{j=1}^{n} W_{i,j}^{w}(\|v_i, v_j\|) \tag{6}$$

$$\aleph_b = \frac{1}{2}\sum_{i=1}^{n}\sum_{j=1}^{n} W_{i,j}^{b}(\|v_i, v_j\|) \tag{7}$$

where $\|.,.\|$ is the Euclidean distance function and

$$W_{i,j}^{w} = \begin{cases} exp\left(\dfrac{\|v_i, v_j\|^2}{\varsigma_i \varsigma_j}\right) * \dfrac{1}{n_k} & \text{iff } v_i \wedge v_j \in C_k \\ 0 & \text{otherwise} \end{cases} \tag{8}$$

$$W_{i,j}^{b} = \begin{cases} exp\left(\dfrac{\|v_i, v_j\|^2}{\varsigma_i \varsigma_j}\right) * \left(\dfrac{1}{n} - \dfrac{1}{n_k}\right) & \text{iff } v_i \wedge v_j \in C_k \\ \dfrac{1}{n} & \text{otherwise} \end{cases} \tag{9}$$

Here, n_k is the membership count of class $\mathbf{C}_k$ and ς_i is the average distance of sample v_i with its k nearest neighbors. The value of k is determined empirically and is set to $k = 7$. This local scaling of affinity matrix caters for multimodal distribution of samples within a given class. The LFDA based coefficient space representation is generated by performing generalized eigenvalue decomposition of $\aleph_b E = \lambda \aleph_w E$ where λ is a generalized eigenvalue and E is the corresponding eigenvector. The enhanced feature space representation of vascular segments, using localized Fisher discriminant directions, is then obtained as:

$$F = \{E_1, E_2, \ldots, E_m\} \tag{10}$$

where $\{E_1, E_2, \ldots, E_m\}$ are eigenvectors arranged in descending order w.r.t. their corresponding eigenvalues $\{\lambda_1, \lambda_2, \ldots, \lambda_m\}$.

The enhanced feature space representation is now used to generate models of different vascular patterns and classification using the generated model. We present a multimodal m-Mediods based modeling and classification approach to suit the expected multimodal distribution of samples within a given vascular pattern. The proposed modelling approach is an extension of our previously proposed m-Mediods based modeling approach as proposed in [9]. Although the approach proposed in [9] can handle patterns with different orientation and scale, it still performs hard classification by classifying sample to a pattern which have a minimum average distance of its k-nearest mediods w.r.t. the test sample. The sample may not lie in the normality region of a pattern to which it is classified but may still lie in the normality range of the mediods belonging to some other class. Such mediods may represent regions of low density and thus having high normality ranges. The hardness of our previously proposed classifier will thus result in the misclassification of such samples. The proposed multimodal m-Mediods based modeling and classification approach targets the problem by proposing a soft classification technique that can handle the above stated problem in the presence of multimodal pattern distribution to minimize misclassification. Given a training data $DB^{(i)}$ containing enhanced feature vector representation of samples belonging to vascular class i, the model of normality is generated using following steps:

1 Initialize learning vector quantization (LVQ) network with $\#_{output}$ neurons. We empirically set $\#_{output} = 3 * m$ upper bounded by the number of segments present in a given class.
2 Initialize weight vectors W_i (where $1 \le i \le \#_{output}$) from the PDF $N(\mu, \Sigma)$ estimated from training samples in $DB^{(i)}$.
3 Determine the winning output node, indexed by c, as:

$$c = \underset{i}{argmin}\ \|W_i, F\| \quad \forall i \tag{11}$$

4 Update the weight vector W_c as:

$$W_c(t+1) = W_c(t) + \alpha(t)\|W_i, F\| \tag{12}$$

where $\alpha(t)$ is the learning rate of LVQ which is decreased exponentially over time t using:

$$\alpha(t) = 1 - e^{(2(t - t_{max}))/t_{max}} \tag{13}$$

where t_{max} is the maximum number of training iterations. We assume $t_{max} = 20{,}000$ lower bounded by the number of training samples. Setting higher values of t_{max} increase computational burden without enhancing the quantization quality.
5 Repeat steps 3 and 4 for all the training iterations.
6 Ignore output neurons with no training sample assigned to it.
7 Identify the closest pair of weight vectors, indexed by (a, b), as:

$$(a, b) = \underset{(i,j)}{argmin}\ \|W_i, W_j\| \times \sqrt{|W_i| + |W_j|} \quad \forall i, j \wedge i \neq j \tag{14}$$

Merge the identified pair of weight vectors as:

$$W_{ab} = \frac{|W_a| \times W_a + |W_b| \times W_b}{|W_a| + |W_b|} \tag{15}$$

where $|.|$ is the membership count function.
8 Iterate through step 7 till the number of weight vectors gets equivalent to m. Append weight vector $\mathbf{W}$ to the list of mediods $\mathbf{M}^{(i)}$ modeling the pattern i.

After the identification of mediods $\mathbf{M}^{(c)}$ for vascular pattern c, we propose to pre-compute a set of possible normality ranges for a given vascular class. Each vascular class will then have a different set of possible normality ranges and each mediod with a modeled pattern will have a different normality range belonging to the pre-computed set depending on the distribution of samples surrounding it. A set of possible normality ranges $\mathbf{D}^{(c)}$ for the vascular class c is pre-computed as follows:

Please cite this article in press as: Usman Akram M, et al. Detection of neovascularization in retinal images using multivariate m-Mediods based classifier. Comput Med Imaging Graph (2013), http://dx.doi.org/10.1016/j.compmedimag.2013.06.008

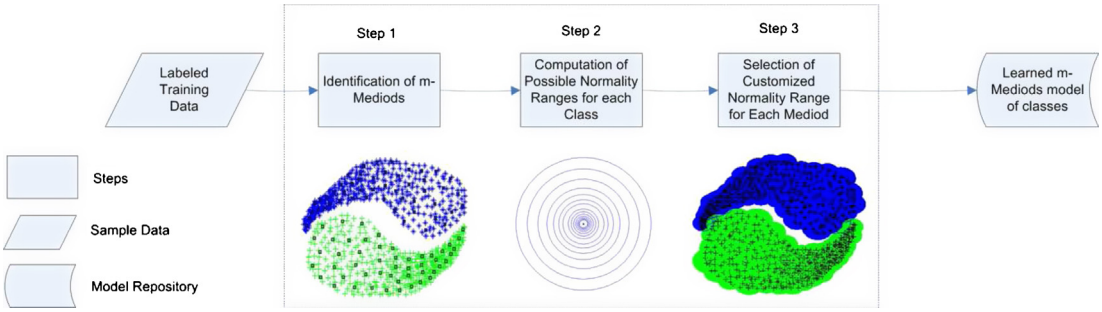

Fig. 7. Simulation of construction of *m*-Mediods based model of normal patterns.

1 Set $\mathbf{D}^{(c)} = \{\}$.
2 Identify the closest pair of mediods (i, j) (indexed by (a, b)) from $\mathbf{M}^{(c)}$ as follows:

$$(a, b) = \underset{(i,j)}{arg\min} \|M_i, M_j\| \quad \forall i, j \wedge i \neq j \tag{16}$$

3 Update $\mathbf{D}^{(c)}$ using

$$\mathbf{D}^{(c)} = \mathbf{D}^{(c)} \cup \{\|M_a, M_b\|\} \tag{17}$$

4 Merge the closest pair of mediods using

$$M_{ab} = \frac{|M_a| \times M_a + |M_b| \times M_b}{|M_a| + |M_b|} \tag{18}$$

5 Iterate through steps 2–4 till the number of mediods gets equivalent to 1.

The possible normality ranges $\mathbf{D}^{(c)}$ for the vascular class c is now used to select customized normality range for each mediod. This is achieved by sequentially passing samples from different classes and identifying the closest mediods w.r.t. these samples. We identify that normality range from $\mathbf{D}^{(c)}$ for a mediod which results in maximum samples from same class to fall in the normality range of that mediod (given it is identified as the closest mediod) while letting minimum samples from other classes to fall in its normality range. Having larger range values will result in correct classification of samples belonging to same class but will also absorb many samples from other classes, thus resulting in false positives. On the other hand, selecting a very tight normality boundary will not only result in rejection of samples belonging to other classes but will also result in rejection of members from same class thus resulting in false negatives. The selection of customized normality range is hence reduced to an optimization problem to select the normality range, from a set of possible normality ranges for a given class, for each mediod that reduces false positives and false negatives. The simulation of modeling process in the presence of multimodal settings is presented in Fig. 7.

Once the mediods and their corresponding normality ranges are identified, the classification of vascular segments using multimodal settings, comprises the following steps:

1 Compute the distance of query segment Q with all the mediods belonging to different classes and sort them in ascending order.
2 Initialize nearest mediod index $\imath$ to 1.
3 Set r to the index of $\imath$th nearest mediod and c to the index of its corresponding class.
4 Classify vascular segment to class c if it lies in the normality range $\imath$th nearest mediod and terminate the classification process.
5 Set $\imath = \imath + 1$.
6 Iterate steps 3–5 till the value of $\imath$ exceeds the total number of mediods in the model. The sample in such extreme case is classified to the class of the nearest mediod in the model.

The proposed classifier is a soft classification approach which caters for the presence of multimodal distributions within and across the vascular patterns. A hard decision of classifying the vascular pattern using *k*-NN classifier would have resulted into some misclassifications. A sample may have been classified to a pattern represented by the majority of mediods from a set of k nearest mediods although it may not be lying in the normality region of a pattern to which it is classified. However, it is likely that it may still fall in the normality region of the second closest but less dense pattern having larger normality range. The proposed soft classification handles this problem by checking for the membership of test sample w.r.t. different vascular classes until it falls into the normality range of some mediod. This phenomena is highlighted in Fig. 8. The samples, represented by 'x' marker, will be classified to blue pattern using a simple hard classification approach. On the other hand, our proposed soft classification technique correctly classifies the sample as normal members of green pattern.

The basic motivation behind proposing a novel multimodal *m*-Mediods based modeling and classification algorithm is to cater for the expected complex, multimodal and overlapping nature of distributions of samples belonging to different classes. Existing commonly used classifiers such as support vector machine (SVM), Gaussian mixture model (GMM) etc are expected to fail in catering for all of the above specified characteristics of expected class distributions. SVM is good at modeling classes with complex but well defined boundaries of class distributions. SVM tends to perform poorly when there is a significant amount of overlap in the class distributions. GMM works well when there is an overlap of classes represented by distinct pdf but is not very good in modeling complex shape classes with complex and tight borders in between them. On the other hand, the proposed multimodal *m*-Mediods classifier is expected to handle all of the above mentioned problems. The issue of multimodal distribution of samples is handled by generating more mediods at locations with dense distribution of samples and vice versa. The normality ranges of mediods are also adjusted w.r.t. density of samples around a given mediod. Mediods at denser locations are expected to have a smaller normality

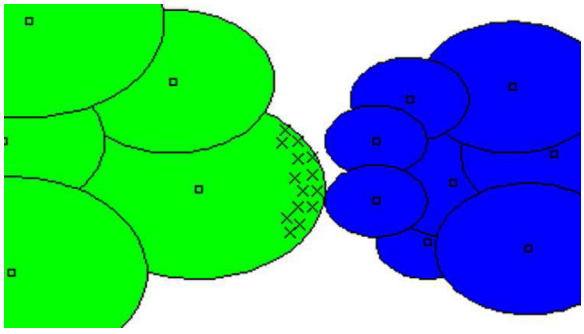

Fig. 8. Soft classification of test samples in the presence of multimodal settings.

Please cite this article in press as: Usman Akram M, et al. Detection of neovascularization in retinal images using multivariate *m*-Mediods based classifier. Comput Med Imaging Graph (2013), http://dx.doi.org/10.1016/j.compmedimag.2013.06.008

range as compared to mediods representing sparse distribution of samples. The location of mediods at different positions of class distribution enables it to model and handle any complex shaped distribution. The overlapping nature of class distribution is handled by employing a soft classifier that caters for the presence of multimodal distributions of overlapping classes. The superiority of our proposed approach as compared to competitors is further validated by performing empirical evaluation in Section 3.

2.6. Grading

Classification stage characterizes each vascular segment as normal or abnormal however the final decision about the input fundus is taken in last phase which is the grading of fundus image. It uses the output of classification to grade retina as healthy or with PDR. Grading phase uses simple set of rules to distinguish between normal and PDR image. The following set of rules are used for grading purposes

- Healthy: No abnormal vascular segment is found.
- PDR: One or more than one vascular segments are classified as abnormal. It further has two categories:
  (a) NVD: One or more abnormal vessels are within the distance of one OD diameter from OD center. For this, the grading phase uses OD coordinates.
  (b) NVE: One or more abnormal blood vessel are found but no one is within the distance of one OD diameter from OD center.

3. Experimental results

3.1. Materials

Databases are tools for evaluation and comparisons of different algorithms and it is really necessary for proper evaluation of medical image processing related algorithms. In order to evaluate algorithms for automated screening and diagnosis of retinal disease, some of benchmark databases are publicly available. The purposes of these databases are to check the validity systems and to compare the results with existing techniques. we use four main retinal image databases for evaluation and comparison of proposed system.

DRIVE (Digital Retinal Images for Vessel Extraction) is a database which has been designed in Netherlands to evaluate and compare different algorithms on vessel segmentation [15]. The images were captured by screening of 400 diabetic patients between 25 and 90 years of age and forty of them have been selected randomly. The images were captured using Canon CR5 non-mydriatic retinal camera with a field of view (FOV) of 45° and a resolution of 768×584.

One of the oldest and mostly used retinal image databases is the STARE (STructured Analysis of REtina) dataset which was designed for structured analysis of retina [31]. There are total 81 retinal images which are acquired using TopCon TRV-50 retinal camera with 35° FOV out of which 30 are from healthy retinal and remaining 51 contain different lesions related to DR. The dataset was firstly used by Hoover et. al. [31] to validate their algorithms and to report their quantitative results. The database contains RBG images with 8 bit per channel and of size 700×605.

DIARETDB (DIAbetic RETinopathy DataBase) is a database which is designed to evaluate automated lesion detection algorithms [32]. It contains 89 retinal images with different retinal abnormalities and provides a best mean to check accuracy of lesions detection. The images are captured with a 50° FOV and a resolution of 1500×1152. Eighty four images out of eighty nine contain different signs of DR and five represent healthy retina.

Table 1
Database description related to PDR.

Database	Images	Normal	With PDR	NVD	NVE
DRIVE	40	19	3	0	3
STARE	81	30	5	3	4
DIARETDB	89	5	7	3	5
MESSIDOR	1200	397	37	27	18

The MESSIDOR is another database which has been established to facilitate computer aided DR lesions detection [30]. The database is collected using TopCon TRC NW6 Non-Mydriatic fundus camera with 45° FOV and resolutions of 1440×960, 2240×1488 and 2304×1536 with 8 bits per color plane. It contains total 1200 images which are divided into three sets of 400 images and each set is further divided into 4 parts to facilitate thorough testing. Each set contains an Excel file with medical findings which can be use for testing purposes. The images are graded into different categories depending on the number and position of lesions.

DRIVE and STARE databases contain manually segmented blood vessels and MESSIDOR database contains image level PDR information about every image. We performed manual segmentation of blood vessels and labeling of images as NVD and NVE with help of two ophthalmologists and an annotation tool developed in MATLAB platform. In addition to image level labeling, the ground truths for classification have also been created with the help of ophthalmologists who marked the vessels as abnormal in order to facilitate the detection of neovascularization. The description about each database which we collected is given in Table 1.

3.2. Results

The evaluation of computer aided diagnostic systems is very important and should be done with great care. We have thoroughly tested our proposed system. The accuracy of PDR detection solely depends on reliable extraction of blood vessels. The performance of vessel segmentation stage is evaluated using ROC curve which is a plot of true positive fraction versus false positive fraction. True positive rate (TPR) is the fraction of number of true positive (pixels that actually belong to vessels) and total number of vessel pixels in the retinal image and false positive rate (FPR) is calculated by dividing false positives (pixels that do not belong to vessels) by total number of non vessel pixels in the retinal image. The detailed comparison analysis of the proposed vessel segmentation technique with existing techniques for DRIVE and STARE databases is given in our previous work [23] and here we have just copied the results in Table 2 for readers understanding.

We have also tested vessel segmentation technique on DIARETDB and MESSIDOR databases by comparing them with manual segmentations from two ophthalmologists and proposed system achieved accuracies of 0.941 and 0.960 respectively. Fig. 9 shows the vascular extraction results for all databases.

The classification of neovascularization is performed using *m*-Mediods based classifier which employs LFDA for feature space enhancement. The transformation matrix obtained by

Table 2
Comparative analysis of blood vessel segmentation.

	DRIVE		STARE	
Method	Az	Acc	Az	Acc
Chaudhuri et al. [18]	0.910	–	0.898	–
Jiang et al. [21]	0.932	0.891	0.929	0.900
Staal et al. [15]	0.952	0.944	0.961	0.951
Soares et al. [16]	0.961	0.946	0.967	0.948
Marin et al. [29]	0.958	0.945	0.976	0.953
Proposed	0.963	0.946	0.970	0.950

Please cite this article in press as: Usman Akram M, et al. Detection of neovascularization in retinal images using multivariate *m*-Mediods based classifier. Comput Med Imaging Graph (2013), http://dx.doi.org/10.1016/j.compmedimag.2013.06.008

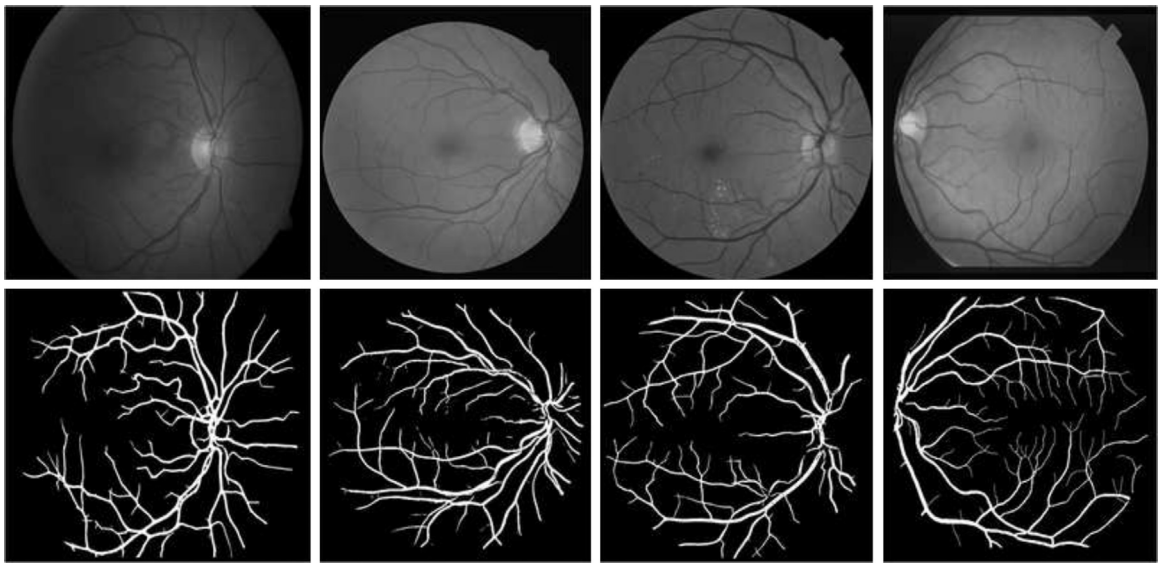

Fig. 9. Vessel segmentation. Row: (1) original retinal images from different databases and (b) extracted vascular pattern using proposed multilayered thresholding technique.

applying LFDA on labeled training data is employed to extract the transformed eigenvectors of original data samples. The same transformation matrix is then applied to test data to obtain the transformed feature space representation that enhances the separation between samples belonging to different classes. Once the transformed feature space representation is generated, it is then used to generate multivariate m-Mediod based models of different classes using transformed feature vector representation. The parameter required for LFDA is the k value which has been set empirically to $k = 7$. The parameter required to be specified for classifier is m i.e. the number of mediods used to model a class. Its value is not sensitive to the performance of classifier given that we specify a reasonably high value for m. We have assumed $m = 70$ if we have training samples greater than 70 else m is set equivalent to the number of training samples for a given class. The parameter t_{max} is the maximum number of training iterations used for coarse

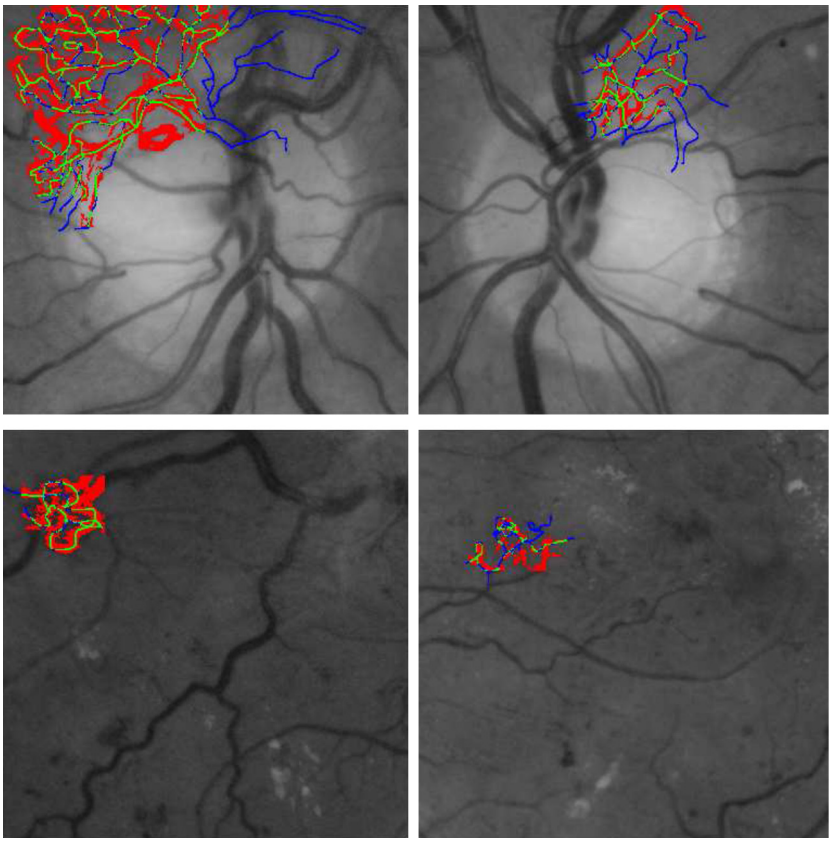

Fig. 10. Segmented abnormal blood vessels and their comparison with manually marked abnormal vessels. Green pixels shows T_P whereas red and blue pixels represent F_P and F_N pixels. (For interpretation of the references to color in this artwork, the reader is referred to the web version of the article.)

Please cite this article in press as: Usman Akram M, et al. Detection of neovascularization in retinal images using multivariate m-Mediods based classifier. Comput Med Imaging Graph (2013), http://dx.doi.org/10.1016/j.compmedimag.2013.06.008

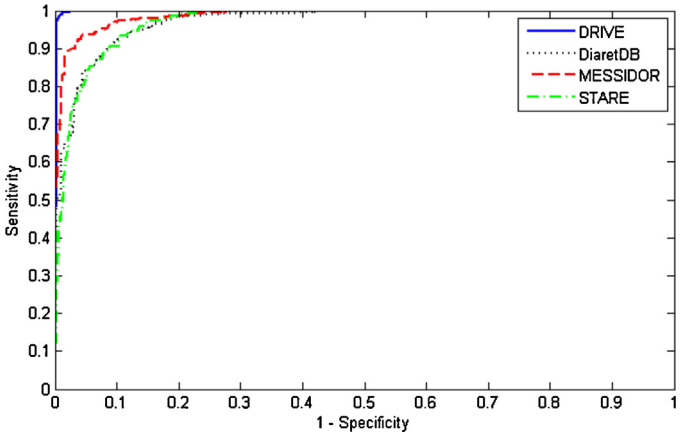

Fig. 11. ROC curve of proposed system for PDR grading on four retinal image databases.

quantization of samples. The algorithm is not at all dependent on the accurate value of t_{max}. Sufficiently high value of t_{max} is good enough to perform quantization of samples. Empirically, setting $t_{max} >= 20{,}000$ gives desirable results. t_{max} is lower bounded by the number of training samples and setting extremely high values for t_{max} results in adding computational burden without enhancing the quality of quantization. The evaluation for abnormal blood vessel detection is done by dividing the data into two sets i.e. training and testing. The division is performed in such a way that training set consists of 70% samples from each class and testing set consists of remaining 30% of data from each class. In order to evaluate the classifier and output of overall system, we have used four parameters for evaluation purposes; i.e. sensitivity (*sen*), specificity (*spec*), accuracy (*acc*) and positive predictive value (*PPV*) given in Eqs. (19)–(22) respectively.

Table 3
Performance evaluation of proposed system for detection of neovascularization.

Database	Sen	Spec	Acc	PPV
DRIVE	1	1	1	1
STARE	0.93	0.98	0.97	0.93
DIARETDB	0.90	0.98	0.97	0.90
MESSIDOR	0.98	0.97	0.98	0.97

$$Sensitivity = \frac{T_P}{T_P + F_N} \tag{19}$$

$$Specificity = \frac{T_N}{T_N + F_P} \tag{20}$$

$$Accuracy = \frac{T_P + T_N}{T_P + T_N + F_P + F_N} \tag{21}$$

$$PPV = \frac{T_P}{T_P + F_P} \tag{22}$$

where

- T_P (true positive): Segments which are classified as healthy and they also belong to healthy vessels in ground truth
- F_P(false positive): Segments which are classified as healthy and they also belong to unhealthy vessels in ground truth
- T_N(true negative): Segments which are classified as unhealthy and they also belong to unhealthy vessels in ground truth
- F_N(false negative): Segments which are classified as unhealthy and they also belong to healthy vessels in ground truth

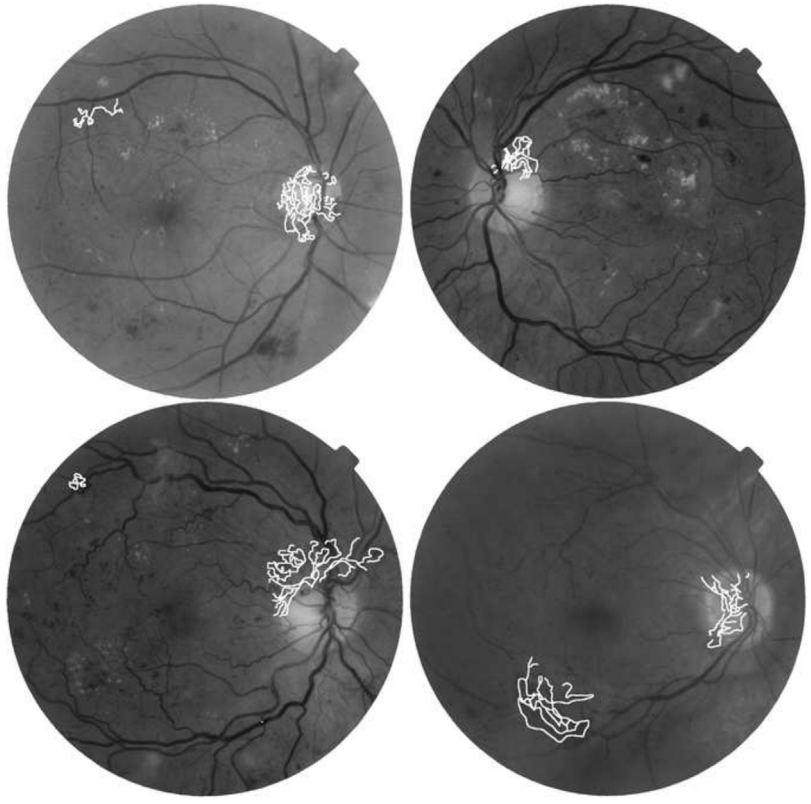

Fig. 12. Fundus images graded as PDR and highlighted abnormal vessels using proposed system.

Please cite this article in press as: Usman Akram M, et al. Detection of neovascularization in retinal images using multivariate *m*-Mediods based classifier. Comput Med Imaging Graph (2013), http://dx.doi.org/10.1016/j.compmedimag.2013.06.008

Table 4
Comparative analysis of proposed classifier with traditional classifiers for classification of NVD and NVE.

	NVD			NVE		
Classifier	Sen	Spec	Acc	Sen	Spec	Acc
*k*NN	0.80	0.78	0.79	0.86	0.85	0.85
GMM	0.93	0.85	0.89	0.92	0.91	0.91
SVM	0.87	0.82	0.84	0.90	0.88	0.89
m-Mediods	0.97	0.92	0.95	0.96	0.94	0.95

Table 3 shows the performance evaluation result for proposed system using all four databases collectively. These experiments are repeated 10 times and the results are averaged to avoid bias in the selection of training and test samples.

Fig. 10 shows the abnormal vessels segmented by proposed system and its comparison with manually labeled abnormal vessels. The original fundus segments are given in Fig. 1(b)–(d). The vessels classified as abnormal by proposed system are marked with red color whereas manually labeled abnormal vessels are highlighted with blue color. Green color show the common pixels in manually and automated segmented abnormal vessels.

The evaluation of proposed system for detection of NVD and NVE is performed at image level and results are computed by matching the results with manual labels which were given in Table 1. The performance of proposed *m*-Mediods based classifier is compared with *k*NN, *SVM* and *GMM* and results are given in Table 4.

The *k*NN is implemented for $k = 7$ and the number of mixtures for GMM are selected as 8 with expectation maximization (EM) for parameter optimization. The SVM is implemented using least square SVM library [33].

The statistical analysis of proposed system is done with the help of receiver operating characteristics (ROC) curves which are plots of true positive rate (sensitivity) versus false positive rate (1 − specificity). This analysis is done for performance evaluation of proposed PDR grading system on different databases. Fig. 11 shows the ROC curves of proposed system for four databases. The system achieves 0.99, 0.97, 0.97 and 0.98 values of area under the curve for DRIVE, STARE, DIARETDB and MESSIDOR respectively.

Fig. 12 shows the some randomly selected fundus images which are graded as PDR by proposed system. Abnormal vessels are highlighted with white color.

4. Conclusion

PDR is an advance stage of DR and can cause severe vision loss. The early and accurate detection of PDR is important and an automated system for detection of PDR can help the ophthalmologists to save patient's vision. This paper proposed a system for early detection and grading of PDR. The system first performed preprocessing to remove background and extracted optic disc coordinates by localizing it. The vascular abnormalities are detected by extracting blood vessels using wavelet transformation and multilayered thresholding technique. The decision for a vascular segment as healthy or unhealthy is done using a multimodel *m*-Mediods based classifier. Finally the proposed system graded the input retinal image as healthy or with PDR and categorized PDR in NVD and NVE. The success of proposed system depends on reliable localization of OD and accurate segmentation of blood vessels for correct grading of PDR as NVD and NVE. Moreover, we can also add tortuosity measure in features for accurate detection of abnormal vessels as they tend to take more tortuous paths than normal vessels.

The main contributions which we have made in this article are (i) a complete system for PDR detection and grading it as NVD or NVE; (ii) a detailed feature set based on properties of normal and abnormal blood vessels is proposed; (iii) a new multimodel *m*-Mediods based classifier is proposed for this problem in order to cater the multivariate distribution of vascular classes. The presented system achieved accuracies of 100%, 97.53%, 97.75% and 98.24% for DRIVE, STARE, DIARETDB and MESSIDOR respectively.

This work presented an improved system for PDR as compared to [11], [12] and [14] in terms of accurate vessel segmentation, feature extraction and classification for both NVD and NVE. It is clear from experiments that proposed classifier detected abnormal vessels more accurately than simple SVM based classifier which was used by [11]. The results have demonstrated that the proposed system can be used in automated detection and grading of proliferative diabetic retinopathy.

References

[1] Klein R, Klein BEK, Moss SE. Visual impairment in diabetes. Ophthalmology 1984;91:1–9.
[2] Sjolie AK, Stephenson J, Aldington S, Kohner E, Janka H, Stevens L, et al. Retinopathy and vision loss in insulin-dependent diabetes in Europe. Ophthalmology 1997;104:252–60.
[3] Effective health care – complications of diabetes. Screening for retinopathy and management of foot ulcers. Royal Society of Medicine Press 1999;5(4).
[4] Ronald PC, Peng TK. A textbook of clinical ophthalmology: a practical guide to disorders of the eyes and their management. 3rd ed. Singapore: World Scientific Publishing Company; 2003.
[5] Kohner EM, Aldington SJ, Stratton IM, Manley SE, Holman RR, Matthews DR. United Kingdom Prospective Diabetes Study, 30: diabetic retinopathy at diagnosis of noninsulin-dependent diabetes mellitus and associated risk factors. Arch Ophthalmol 1998;116:297–303.
[6] Quellec G, Russell Stephen R, Abrmoff Michael D. Optimal filter framework for automated, instantaneous detection of lesions in retinal images. IEEE Trans Med Imaging 2011;30(2):523–33.
[7] Akram MU, Khan SA. Automated detection of dark and bright lesions in retinal images for early detection of diabetic retinopathy. J Med Syst 2012;36(5):3151–62.
[8] Akram MU, Tariq A, Anjum MA, Javed MY. Automated detection of exudates in colored retinal images for diagnosis of diabetic retinopathy. OSA J Appl Opt 2012;51(20):4858–66.
[9] Akram MU, Khalid S, Khan SA. Identification and classification of microaneurysms for early detection of diabetic retinopathy. Pattern Recogn 2013;46(1):107–16.
[10] Niemeijer M, Abrmoff MD, Ginneken BV. Information fusion for diabetic retinopathy CAD in digital color fundus photographs. IEEE Trans Med Imaging 2009;28(5):775–85.
[11] Goatman KA, Fleming AD, Philip S, Williams GJ, Olson JA, Sharp PF. Detection of new vessels on the optic disc using retinal photographs. IEEE Trans Med Imaging 2011;30(4):972–9.
[12] Agurto C, Murray V, Barriga E, Murillo S, Pattichis M, Davis H, et al. Multiscale AM–FM methods for diabetic retinopathy lesion detection. IEEE Trans Med Imaging 2010;29(2):502–12.
[13] Jelinek HF, Cree MJ, Leandro JJG, Soares Jr JVBRMC, Luckie A. Automated segmentation of retinal blood vessels and identification of proliferative diabetic retinopathy. J Opt Soc Am A 2007;24:1448–56.
[14] Nayak J, Bhat PS, Acharya R, Lim UCM, Kagathi M. Automated identification of diabetic retinopathy stages using digital fundus images. J Med Syst 2008;32:107–15.
[15] Staal JJ, Abramoff MD, Niemeijer M, Viergever MA, van Ginneken B.Ridge based vessel segmentation in color images of the retina. IEEE Trans Med Imaging 2004;23(4):501–9.
[16] Soares JVB, Leandro JJG, Cesar Jr RM, Jelinek HF, Cree MJ. Retinal vessel segmentation using the 2D Gabor wavelet and supervised classification. IEEE Trans Med Imaging 2006;25(9):1214–22.
[17] Yen GG, Leong W-F. A sorting system for hierarchical grading of diabetic fundus images: a preliminary study. IEEE Trans Inf Technol Biomed 2008;12(1):118–30.
[18] Chaudhuri S, Chatterjee S, Katz N, Nelson M, Goldbaum M. Detection of blood vessels in retinal images using two-dimensional matched filters. IEEE Trans Med Imaging 1989;8(3):263–9.
[19] Hoover A, Kouznetsova V, Goldbaum M. Locating blood vessels in retinal images by piecewise threshold probing of a matched filter response. IEEE Trans Med Imaging 2000;19(3):203–10.
[20] Mendonca AM, Campilho A. Segmentation of retinal blood vessels by combining the detection of centerlines and morphological reconstruction. IEEE Trans Med Imaging 2006;25(9):1200–13.
[21] Jiang X, Mojon D. Adaptive local thresholding by verification based multithreshold probing with application to vessel detection in retinal images. IEEE Trans Pattern Anal Mach Intell 2003;25(January(1)):131–7.
[22] Antoine JP, Carette P, Murenzi R, Piette B.Image analysis with two-dimensional continuous wavelet transform. Signal Process 1993;31(3):241–72.
[23] Akram MU, Khan SA. Multilayered thresholding-based blood vessel segmentation for screening of diabetic retinopathy. Eng Comput 2013;29(2):165–73.

Please cite this article in press as: Usman Akram M, et al. Detection of neovascularization in retinal images using multivariate *m*-Mediods based classifier. Comput Med Imaging Graph (2013), http://dx.doi.org/10.1016/j.compmedimag.2013.06.008

[24] Tariq A, Akram MU. An automated system for colored retinal image background and noise segmentation. In: IEEE symposium on industrial electronics and applications (ISIEA 2010). 2010. p. 405–9.
[25] Akram MU, Khan A, Iqbal K, Butt WH. Retinal images: optic disk localization and detection. In: ICIAR 2010, Part II, LNCS 6112. 2010. p. 40–9.
[26] Gonzalez RC, Woods RE. Digital image processing. 2nd ed. Prentice hall; 2002.
[29] Marín D, Aquino A, Emilio MGA, Bravo JM. A new supervised method for blood vessel segmentation in retinal images by using gray-level and moment invariants-based features. IEEE Trans Med Imaging 2011;30(1).
[30] MESSIDOR;1; http://messidor.crihan.fr/index-en.php
[31] Hoover, STARE database,;1; http://www.ces.clemson.edu/ahoover/stare
[32] Kauppi T, Kalesnykiene V, Kamarainen J-K, Lensu L, Sorri I, Raninen A, Voutilainen R, Uusitalo H, Kälviä inen H, Pietilä J. DIARETDB1 diabetic retinopathy database and evaluation protocol. In: Technical report. 2006.
[33] Least square support vector machine;1; http://www.esat.kuleuven.be/sista/lssvmlab/

Usman Akram is an assistant professor in college of Electrical & Mechanical Engineering, National University of Sciences & Technology, Pakistan. He Holds a PhD degree in Computer Engineering with specialization in medical image analysis and is among the youngest PhDs in Pakistan. His research areas are image/signal processing, biometrics, medical image analysis and pattern recognition. He is a recipient of different national and international awards such as P@SHA 2012, APICTA 2012, Travel fellowships, cash awards on journal publications, commandant's plaque of excellence. Currently he is working on implementation of a telescreening system for diagnosis of diabetic retinopathy in coordination with Shifa International Hospital and AFIO (Armed Forces Institute of Ophthalmology), Pakistan.

Shehzad Khalid graduated from Ghulam Ishaq Khan Institute of Engineering Sciences and Technology, Pakistan, in 2000. He received the M.Sc. degree from National University of Science and Technology, Pakistan, in 2003 and the Ph.D. degree from the University of Manchester, U.K., in 2009. He is currently an assistant professor at the Bahria University of Management and Computer Sciences, Pakistan. His research interests include: dimensionality reduction, indexing and retrieval, profiling and classification, trajectory-based motion learning profiling and classification, computer vision, machine learning.

Anam Tariq has M.S. degree in computer engineering from National University of sciences and technology. She has a number of research publications in medical image processing. Her research interest includes image processing, biometrics and pattern recognition.

M. Younus Javed has a Ph.D. degree and he is currently acting as dean, College of Electrical & Mechanical Engineering, National University of Sciences and Technology. He has a large number of publications in field of image processing, biometrics, software engineering and communication.

Please cite this article in press as: Usman Akram M, et al. Detection of neovascularization in retinal images using multivariate *m*-Mediods based classifier. Comput Med Imaging Graph (2013), http://dx.doi.org/10.1016/j.compmedimag.2013.06.008